



Ni⁺² permease system of *Helicobacter pylori* contains highly conserved G-quadruplex motifs

Uma Shankar^a, Subodh Kumar Mishra^a, Neha Jain^a, Arpita Tawani^a, Puja Yadav^b,
Amit Kumar^{a,*}

^a Department of Biosciences and Biomedical Engineering Indore, Simrol, Indore, Madhya Pradesh 455235, India

^b Department of Microbiology, Central University of Haryana, Mahendgarh, Haryana, India

ARTICLE INFO

Keywords:

Antimicrobial resistance
G-quadruplex motif
Helicobacter pylori
Nickel transporter genes
Nucleic acid

ABSTRACT

The genome of a micro-organism contains all the information required for its survival inside its host cells. The guanine rich regions of the genome can form stable G-quadruplex structures that act as the regulators of gene expression. Herein, the completely sequenced genomes of *Helicobacter pylori* were explored for the identification and characterization of the conserved G-quadruplex motifs in this gastrointestinal pathogen. Initial *in silico* analysis revealed the presence of ~8241 GQ motifs in the *H. pylori* genome. Metal binding proteins of *H. pylori* are significantly enriched in the GQ motifs. Our study emphasizes the identification and characterization of four highly conserved G-quadruplex forming motifs (HPGQs) in the nickel transporter genes (*nixA*, *niuB1*, *niuB2*, and *niuD*) of the *H. pylori*. Nickel is a virulence determinant in *H. pylori* and is required as a co-factor for the urease and [NiFe] hydrogenase enzymes that are crucial for its survival in the stomach lining of humans. The presence of GQ motifs in these nickel transporter genes can affect their expression and may alter the functioning of Urease and [NiFe] hydrogenase. Similar to human and virus G-quadruplexes, targeting these conserved PGOs with bioactive molecules may represent a novel therapeutic avenue for combating infection of *H. pylori*. The identified HPGQs were characterized *in-vitro* by using CD spectroscopy, electrophoresis technique, and NMR spectroscopy at both acidic (4.5) and neutral pH (7.0). ITC revealed the specific interaction of these HPGQs with high affinity to the known G-quadruplex binding ligand, TMPyP4. The mTFP based reporter assay showed decrease in the gene expression of mTFP in the TMPyP4 treated cells as compared to the untreated and further affirmed the formation of stable G-quadruplex structures in the HPGQ motifs *in vivo*. This is the first report for characterizing G-quadruplex motifs in nickel transport-associated genes in the *H. pylori* bacterium.

1. Introduction

H. pylori is a gram-negative, spiral-shaped, microaerophilic bacteria estimated to infect approximately 50% of the world's human population (Backert et al., 2016; Hooi et al., 2017). In 2015, the global prevalence of the *H. pylori*-infected people was estimated as 4.4 billion individuals across the world (Hooi et al., 2017). The prevalence of *H. pylori* is higher in developing countries, ranging from ~85% to 95% compared to that in developed countries (30–50%), as its occurrence largely depends on the socio-economic and hygienic conditions (Alsulaimany et al., 2020). The prevalence of *H. pylori*-infected people is higher in the African (79.1%), Latin American and the Caribbean (63.4%), and Asian (54.7%) populations (Hooi et al., 2017). It causes chronic gastritis, peptic ulcer disease, MALT lymphoma, and gastric adenocarcinoma in the infected

person (Backert et al., 2016). Gastric cancers rank second in terms of mortality among all the cancers, and 89% of these gastric cancers occur as a consequence of *H. pylori* infection (Alsulaimany et al., 2020). *H. pylori* can survive in the varied pH range of 4–8 (Sidebotham et al., 2003). It lives in the stomach with an acidic pH, and for colonizing and growth, it moves to the mucus lining that has the neutral pH. Its unique feature of producing a urease enzyme that maintains the pH homeostasis inside the bacterium helps it to survive in the low pH range. The long-term persistence of this bacteria in the stomach linings results in the release of several virulence factors like the vacuolating cytotoxin A (VacA), Cag A, peptidoglycans, adhesins, and outer membrane pore-forming proteins (OMPs) that trigger cell signaling pathways leading to gastric carcinogenesis (Wróblewski et al., 2010).

Considering the high prevalence rate of *H. pylori* infection across the

* Corresponding author.

E-mail address: amitk@iiti.ac.in (A. Kumar).

<https://doi.org/10.1016/j.meegid.2022.105298>

Received 20 June 2021; Received in revised form 30 March 2022; Accepted 2 May 2022

Available online 5 May 2022

1567-1348/© 2022 The Authors. Published by Elsevier B.V. This is an open access article under the CC BY-NC-ND license (<http://creativecommons.org/licenses/by-nc-nd/4.0/>).

world population, it becomes indispensable to develop a propitious therapeutic approach against its infection. Antimicrobial resistance (AMR) against *H. pylori* has constantly been increasing throughout the world. According to the reports, different first-line antibiotics contribute to the drug resistance with metronidazole contributing the highest with 47.2% of the AMR followed by clarithromycin (19.7%), then levofloxacin (18.9%), amoxicillin (14.7%), and rifampicin (6.7%) (Domonovich-Asor et al., 2021). This rapid emergence of drug resistance is the consequence of mutations in various genes at the genome level. For example, three-substitution mutations at the 2142th nucleotide (A → G or A → C) and 2143th nucleotide (A → G) positions of the *H. pylori* genome causes conformational changes in the peptidyl transferase loop of the 23S rRNA gene (Mégraud, 2012). This results in the decreased binding affinity of clarithromycin to its target site and resistance of bacteria to clarithromycin (Mégraud, 2012). Usually, such kind of mutations occur by chance in the bacterial life cycle and persist in the bacterial genome for many generations leading to drug resistance (Mégraud, 2012). Therefore, identification of the evolutionarily conserved site in the bacterial genome and assessment of their drug-ability becomes the urgent and unmet need for countering the infection of *H. pylori*.

The G-quadruplex structure forming conserved nucleic acid motifs has been revealed to be orchestrated throughout the genome of various organisms that includes both eukaryotes as well as prokaryotes (Murat and Balasubramanian, 2014; Yadav et al., 2021; Wu et al., 2021). G-quadruplex motifs are evolutionarily conserved motifs and appeared to be novel transcriptional regulator that helps the higher organisms in multiple physiological activities (Wu et al., 2021). In humans, G-quadruplex structure plays a vital role in various biological processes such as regulation of telomerase activity, genome stability, expression of various oncogenes, etc. (Rhodes and Lipps, 2015). The demonstration of G-quadruplex DNA structures in the telomeres and their importance in cancer growth and progression has revealed them as a potent drug targets for anti-cancer therapy (Shalaby et al., 2013; Awadasseid et al., 2021). G-quadruplexes reported in nuclease hypersensitive elements in promoter regions of various proto-oncogenes such as KRAS, *c-myc*, etc., play a regulatory role in the transcriptional activity of these oncogenes and revealed as a promising drug target for potent anti-cancer therapeutics (Awadasseid et al., 2021; Chen et al., 2014; Huang et al., 2006; Tawani et al., 2016; Tawani et al., 2017; Pandya et al., 2021).

Various pathogens are also evaluated for the presence of G-quadruplex motifs in their genome. A recent study showed a strong correlation between the G-quadruplex motifs of double-stranded viruses and their respective bacterial host depicting their coevolution (Bohálová et al., 2021). G-quadruplexes are also reported to be enriched in the promoter regions of viruses and might play a critical role in their pathogenesis (Ruggiero et al., 2019; Bohálová et al., 2021). In the case of human pathogens (such as viruses and bacteria), viral genomes have been more explored for conserved G-quadruplex drug targets (Ruggiero and Richter, 2018). For instance, the stabilization of the G-quadruplex forming motif present in the long terminal repeat of the human immunodeficiency virus (HIV) genome results in the inhibited viral DNA replication (Ruggiero and Richter, 2018; Perrone et al., 2014). The Epstein-Barr virus (EBV) had been observed to utilize a conserved G-quadruplex motif present in the mRNA of the EBNA1 protein for escaping itself from the host immune system. The modulation of the G-quadruplex structure by small molecules increased the expression of the EBNA1 protein and reduced the immuno-recognition mechanism of the host (Ruggiero and Richter, 2018; Lista et al., 2017). The G-quadruplex present in the oriLyt-R, oriLyt-L, and K5–9, v-IRF2, and v-IRF3 genes in the Kaposi's sarcoma-associated herpesvirus (KSHV) virus was observed to play a vital role in its latency (Madireddy et al., 2016). The highly infectious influenza strain, H1N1 showed the presence of various G-quadruplex motifs that can be further explored for developing novel therapeutic approaches (Brázda et al., 2021).

Similarly, the coding region of several essential genes (prM, E, NS1,

NS3, NS5) of Zika virus genome and Pac1 signal of human herpesvirus (HSV) revealed to contain G-quadruplex forming motifs (Fleming et al., 2016; Biswas et al., 2018). Recently, our group has shown that G-quadruplex stabilizing ligands like Braco-19 and TMPyP4 can significantly inhibit the Zika virus replication and, thereby emphasizing the involvement of G-quadruplexes in the replication, transcription, and translation regulation of the viral genome (Majee et al., 2021). TMPyP4 also showed anti-viral activity against HSV-1 and regulate its replication inside the host cells (Artusi and Ruggiero, 2021). Other studies revealed the presence of G-quadruplex motifs in the genome of Nipah (Majee et al., 2020a) and Adenovirus (Majee et al., 2020b). These studies have convincingly suggested the presence of G-quadruplex in the viral genome that can be explored as a promising drug target for the anti-viral therapy (Ruggiero and Richter, 2018). The Nidovirale family that included the recently emerged highly pathogenic SARS-CoV-2 also harbors evolutionary conserved G-quadruplex motifs in their genomes and are promising anti-viral drug targets (Bartas et al., 2020).

Similar to human and viral G-quadruplexes, archaeobacterial and eubacterial genomes are also investigated for the presence of G-quadruplex forming motifs that are involved in their growth and pathogenesis (Holder and Hartig, 2014; Endoh et al., 2013; Bartas et al., 2019; Dey et al., 2021). For example, the human pathogen *Neisseria gonorrhoeae* has been shown to evade the human immune system by antigenic variation in the pilin (*pilE*) gene. This antigenic variation process is regulated by the G-quadruplex structure forming motif located upstream of the *pilE* gene (Cahoon and Seifert, 2009). A recent study also demonstrated enrichment of G-quadruplexes in the cis-regulatory regions of the pathogenic bacteria (Dey et al., 2021). Apart from cis-regulatory regions, various G-quadruplexes are reported in the open-reading frames of essential genes in various bacteria. The *mce1R* operon, gene encode for PE_PGRS family, Glucose-6-phosphate dehydrogenase 1 (*zwf1*), oxidation-sensing regulator transcription factor (*mosR*), membrane NADH dehydrogenase (*ndhA*), and an ATP-dependent Clp protease (*clpX*) in *Mycobacterium tuberculosis* genome contains potential G-quadruplex motifs (Perrone et al., 2017a). Another study revealed the presence of conserved G-quadruplex motifs in the *espB*, *espK*, and *cyp51* genes of *M. tuberculosis* (Mishra et al., 2019). All these genes showed to play an active role in providing virulence to the bacteria inside the host cell. Targeting these G-quadruplex motifs by G4 selective small molecules has been shown to reduce the expression of the harbored gene and the survival of the bacteria (Perrone et al., 2017b; Thakur et al., 2014). The genomes of *Vibrio cholera* (Shankar et al., 2020a), *Salmonella enterica* (Jain et al., 2020), *Klebsiella pneumoniae* (Shankar et al., 2020b), and *Neisseria meningitidis* (Jain and Shankar, 2022) have also shown the presence of conserved G-quadruplex motifs that regulates the harbored gene expression. A recent study showed the enrichment of potential G-quadruplex forming motifs (PGOs) in the genomes of thermophilic bacteria and stress-resistant *Deinococcus* bacteria (Ding et al., 2018) that folds into stable G-quadruplex conformation *in-vitro*. A G-quadruplex motif located in the promoter region of the *nasT* gene of *Paracoccus denitrificans* regulates the assimilatory nitrate/nitrites reductase system (Waller et al., 2016).

In some of the viruses and bacterial cell, various proteins are also reported to be involved in regulating the G-quadruplex motif/structure/functions. The interaction of RecA recombinase with the G-quadruplex motif is essential for antigenic variation in *N. gonorrhoeae* (Kuryavyi et al., 2012). Likewise, in *M. tuberculosis*, UvrD1 and UvrD2 helicases unwinds the G-quadruplex structures during replication and transcriptional processes (Saha et al., 2019). The nucleocapsid protein of HIV-1 unfolds the stable G-quadruplexes structures and helps in viral genome amplification, which can be abrogated by G-quadruplex binding ligands (Butovskaya et al., 2019). Besides pathogen proteins, various host proteins also interact with the viral G-quadruplexes and play a critical role in pathogenesis. The host protein, Nucleolin (NCL), interacts with the G-quadruplexes located in the EBNA1 mRNA and helps in the viral immune escape by inhibiting its expression leading to a decrease in the

antigen presentation. The addition of G4-binding ligand, PhenDC3 abrogated the NCL-G-quadruplex interactions and increases the antigen presentation (Reznichenko et al., 2019). Similarly, the CNBP protein unfolds the G-quadruplex motifs present in the genome of SARS-CoV-2 (Bezzi et al., 2021).

Considering the presence of G-quadruplex motifs and their regulatory function in other human pathogens, we sought to explore the potential G-quadruplex forming motifs (HPGQs) in the *H. pylori* genome. To the best of our knowledge, it is the first study that reports the presence of PGQs in the four essential genes: *nixA*, *niuB1*, *niuB2* and *niuD* of the *H. pylori* genome. These genes encode for essential proteins that participate in the nickel transportation system of the bacteria (Fischer et al., 2016). Nickel acts as a virulence determining factor for the *H. pylori* by working as a co-factor for various essential enzymes of the bacteria, like urease [NiFe] hydrogenase, Ni-SOD and CO dehydrogenase and other enzymes involved in nitrogen metabolism and detoxification (de Reuse et al., 2013a). Urease and [NiFe] hydrogenase are required for the colonization and survival of the bacteria in the low pH environment of the host (de Reuse et al., 2013a). The formation of the G-quadruplex structure in these genes have been confirmed by the circular dichroism spectroscopy (CD), nuclear magnetic resonance (NMR), and electrophoretic mobility shift assay (EMSA) techniques. The high affinity of TMPyP4, a G-quadruplex binder to this HPGQs by ITC and decreased expression of the mTFP reporter gene in the presence of the ligand further affirmed the formation of G-quadruplex conformation in this HPGQs.

2. Materials and methods

2.1. Prediction of the G-quadruplex forming sequences in *H. pylori* genome

All the completely sequenced genome of *H. pylori* including *H. pylori* 26695 were fetched from the Nucleotide database available at National Center for Biotechnology Information (NCBI). The obtained sequences were then processed to mine potential G-quadruplex (PGQ) forming sequences using an in-house G-quadruplex prediction tool (Mishra et al., 2016) and an outsourced Quadparser (Huppert and Balasubramanian, 2005). This in-house tool used the following regular expression to search PGQ sequences in the *H. pylori* genomes:

$$G_{\{Y1\}}[X]_{\{Y2\}}G_{\{Y1\}}[X]_{\{Y2\}}G_{\{Y1\}}[X]_{\{Y2\}}G_{\{Y1\}}$$

Where, X corresponds to any nucleic acid base including A, G, C, and T, while Y1 corresponds to the length of consecutive G tract and can be any integer between 2 to 7, and Y2 corresponds for variable loop length and can be any integer number between 1 to 20. The maximum length for the predicted HPGQ was kept 45 bases. While the Quadparser uses the below regular expression:

$$'([gG]\{2,\}\w\{1,20\})\{3,\}[gG]\{2\}')$$

Where g/G stands for guanine and w stands for any nucleotide. The algorithm of this tool searches the putative G-quadruplex forming sequences in both the sense and antisense strands. All the predictions were listed and examined for their location from the GenBank sequence database. We also used the G4Hunter tool based on GC skewness (Brázda et al., 2019) and PENGUINN tool based on Neural Network (Klimentova et al., 2020) for the comparative analysis. These prediction results were further confirmed by other available tool QGRS mapper (Kikin et al., 2006; Dhapola and Chowdhury, 2016).

The frequency of the predicted PGQs in all the available strains was calculated manually using NCBI BLAST, and consensus sequences were generated using the WebLogo tool by aligning 5 bp upstream and downstream of the predicted motif.

2.2. Mapping of G4 motifs on the *H. pylori* genome

The obtained PGQ sequences were mapped for their location on the *H. pylori* genome using the coordinates extracted from G4 prediction tools. For constructing the circular genomic map, the ShinyCircos server (Yu et al., 2018) was used. For the functional annotation of HPGQs Graphics mode of the GenBank database was explored. The HPGQs coming in the ORF region were termed genic, while those in between the ORFs were annotated as intergenic GQ motifs. The gene enrichment analysis of the HPGQ harboring genes was performed using DAVID (Huang da et al., 2009a; Huang da et al., 2009b).

2.3. DNA sample preparation

DNA sequences were procured from Sigma Aldrich, 100 µM stock solutions in MQ water were prepared according to the manufacturer protocol. Prior to each experiment, DNA oligonucleotides were heated at 92 °C for 10 min and allowed to reanneal slowly at room temperature for 2 h. All the oligonucleotides were further dissolved in four different Tris buffer (pH = 7.0, 10 mM) and ammonium acetate buffer (pH = 4.5, 10 mM) containing 50 mM of 4 different cations K⁺, Na⁺, Mg²⁺ and Li⁺ separately.

2.4. Circular dichroism and melting experiment

All CD spectra were observed at 25 °C at a 20 nm/min rate, using Jasco J-815 Spectropolarimeter (Jasco Hachioji, Tokyo, Japan) equipped with Peltier junction temperature controller. A constant supply of nitrogen gas was provided to avoid the water condensation around the cuvette. A cuvette of 0.2 cm path length was used, and a spectra scan of each sample was recorded. For melting studies, data were collected at a wavelength of higher strength for CD signal and scanned for a temperature range of 25 °C to 98 °C for each PGQ sequence in all the four cations containing buffers.

2.5. Gel mobility shift assay

Gel mobility shift assay was performed using 30% native polyacrylamide gel using 1 × TBE buffer. Each sample was dissolved in either ammonium acetate (pH = 4.5, 10 mM) buffer containing four different cations K⁺, Na⁺, Mg²⁺, Li⁺ (50 mM each) separately. 20 µM of DNA was loaded, and for each sample, a similar length of DNA oligonucleotides was taken as a negative control, and a single standard G-quadruplex (Tel22 DNA) was taken as a positive control. All the experiments were performed at 4 °C, maintaining the voltage at 90 in a vertical gel unit system.

2.6. Nuclear magnetic resonance

NMR experiments were conducted using AVANCE 400 MHz BioSpin International AG, Switzerland, equipped with a 5 mm broadband inverse probe (BBI). Topspin (1.3 version) software was used for the NMR data processing and analysis. 3-(Trimethylsilyl) propionic-2, 2, 3, 3-D4 acid sodium salt (TSP) was taken as a reference compound. All the NMR spectra were performed using H₂O/D₂O solvent at a 9:1 ratio and at a temperature of 298K with 20 ppm spectral width. All the samples were heated at 92 °C and kept at room temperature for reannealing.

2.7. Isothermal titration calorimetry (ITC)

ITC analysis was performed using a MicroCal iTC200 isothermal titration calorimeter (GE Healthcare) at 25 °C. HPGQ oligonucleotides (20 µM) were dissolved in 10 mM potassium buffer (pH = 7.2). 200 µM stock solution of TMPyP4 was prepared in the same buffer condition. 21 injections of the 1.80 µL of TMPyP4 (200 µM) was added at each step from the syringe into the cell of the calorimeter containing 20 µM G-

quadruplex DNA. The duration of each injection was set as 3.6 s, and spacing between each successive injection was fixed at 90s. Oligonucleotides' heats of dilution were determined by injecting the same concentration of TMPyP4 into the potassium phosphate buffer and subtracting it from the binding isotherms before curve fitting. Data were acquired and analyzed by using the origin scientific software version 7 (MicroCal Software Inc.) to generate thermograms. As ligand might interact with the G-quadruplex either *via* stacking mode of interaction or by loop binding, the thermograms were fitted in the two set of sites binding model to determine association constant (K_a) values.

2.8. mTFP reporter assay

The HPGQ motif sequences were cloned at the upstream region of the mTFP gene in pCAG-mTFP plasmid by using overlap extension PCR. One plasmid with a mutant GQ motif that was unable to fold into GQ conformation was also constructed as a negative control. The primers used for the cloning are enlisted in Supplementary Table S2. The PCR amplified product was treated with *DpnI* enzyme to cleave the methylated parent pCAG-plasmid while retaining the amplified PCR product. Thereafter, the product was ligated and transformed into *E.coli* DH5 α cells and selected by using ampicillin resistance. The positive colonies were picked and grown overnight for plasmid purification using the

HiMedia Midi-prep Plasmid isolation kit.

HEK293T cells were grown in a six-well plate were transfected with pCAG-GQ-mTFP and pCAG-mutant-GQ plasmids by using the Calcium chloride method. The cells were treated with 10 μ M and 20 μ M TMPyP4 molecule, the untreated ones were considered as control, and mTFP fluorescence was observed in Olympus Confocal Microscopy.

3. Results

3.1. Identification of putative G-quadruplex sequences

Considering the *in vivo* formation of a G-quadruplex structure requires four sets of at least two consecutive guanines with the gap of at least one loop forming nucleotide (Ruggiero and Richter, 2018), here we searched for the potential G-quadruplex forming motifs (HPGQs) in the genome of *H. pylori* 26695 (NCBI accession ID: NC_000915.1). To obtain the HPGQs data, we employed our previously developed G4 prediction tool and Quadparser tool (Supplementary File S2) (Mishra et al., 2016). Both these tools are pattern based and provided similar results with four-variable guanine tracts joined by variable-length nucleotide stretches. As the bacterial genome encodes the protein using both strands, we also analyzed the presence of GQ motifs in both sense and antisense strands of the bacterial genome. GQ prediction with the parameter of G-tract ≥ 2

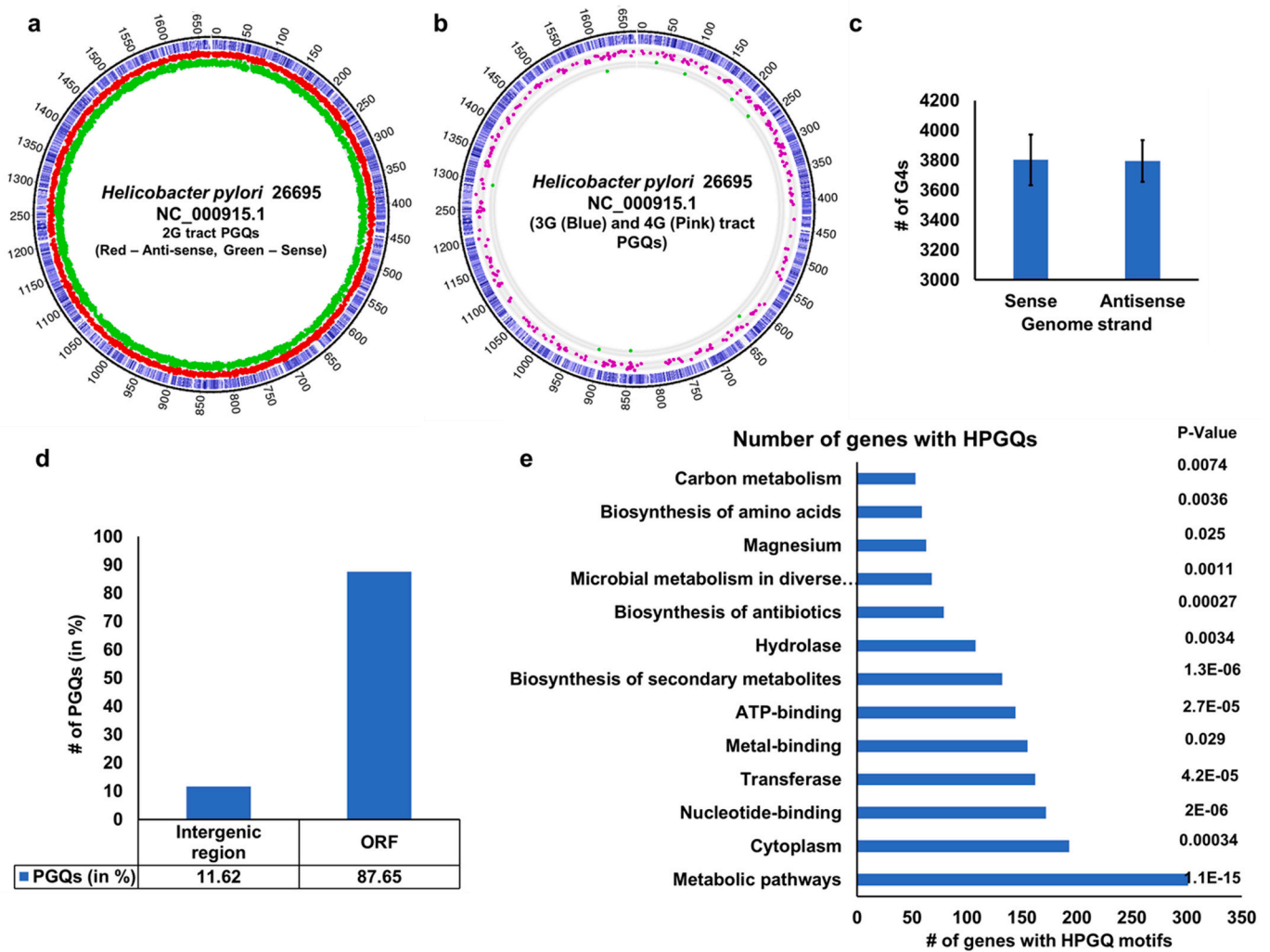


Fig. 1. G-quadruplex motifs in the *Helicobacter pylori* 26,695 genome. (a) G-quadruplex motifs with the G-tract ≥ 2 and loop length ≤ 20 bases. Red points denote HPGQs in the sense strand, while green represents in the antisense strand. (b) G-quadruplex motifs in *H. pylori* 26,695 with G-tract ≥ 3 (purple) and G-tract ≥ 4 (Green). The loop length was kept constant and was ≤ 20 bases. (c) Number of G-quadruplex motifs (in %) in the open reading frames or in the intergenic region. (For interpretation of the references to colour in this figure legend, the reader is referred to the web version of this article.)

and a loop length ≤ 20 revealed the presence of 8241 putative motifs in the genome of *H. pylori* 26,695. This shows the presence of a highly GQ enriched genome of *H. pylori* with an average density of 4.95 GQs/Kb in a low GC-rich genome ($\sim 38.9\%$). Out of these, 4064 were located in the sense strand, while 4177 motifs were present in the antisense strand (Fig. 1a). We also checked the presence of higher order GQ motifs in the *H. pylori* genome and observed the presence of 281 GQ motifs with the G-tract ≥ 3 while only nine GQ motifs with the G-tract of ≥ 4 (Fig. 1b). On annotating the PGQ motifs with two G-tracts, we observed 957 ($\sim 11\%$) GQ in the intergenic region while 7223 GQ ($\sim 89\%$) motifs were located in the open reading frames of various protein coding genes (Fig. 1c). Almost equal number of G-quadruplex motifs were located in the positive strand and the negative strand of the *H. pylori* genomes depicting no significant strand biases (Fig. 1d).

We also employed two more G-quadruplex prediction tools: G4Hunter that is based on GC skewness, and PENGUINN, a machine learning-based tool for analyzing the HPGQs in the *H. pylori* genome (Supplementary Fig. S1). G4Hunter predicts G-quadruplex motifs with a maximum window size of 25 and varied thresholds. With 1.2 thresholds, *H. pylori* 26,695 genome showed the presence of 21,144 HPGQs, while 1.4 thresholds highlighted the formation of 8606 motifs. Likewise, with thresholds 1.6, 1.8 and 2.0, 3298, 1160, 405 GQ motif were predicted respectively. PENGUINN tool is based on Convolutional neural networks that accurately predict the G-quadruplexes than the classical tools. The HPGQ motifs predicted by our in-house script provided a PENGUINN score in the range of 0.2–0.99, highlighting the presence of both low and high propensity of GQ formation *in-vitro* (Supplementary File S2). Both of these tools also highlighted the presence of HPGQ motifs in the *H. pylori* genome that have a high propensity to form G-quadruplexes *in-vitro* and *in-vivo*.

All the HPGQ harboring genes of *H. pylori* were then functionally

clustered using the DAVID tool. The maximum number of HPGQs were present in the genes involved in various metabolic pathways, followed by nucleotide-binding proteins and transferases. Another significant class with HPGQ enrichment was that of metal binding proteins (Fig. 1e). Metal binding proteins play a critical role in colonization in the human gastric lumen and help in immune escape. In the host environment, the presence and absence of various metal ions, including nickel, iron, copper, and zinc influences the gene expression in *H. pylori* that impacts the bacterial persistence. Nickel is important for the activation of Urease and [NiFe] dehydrogenase, two enzymes critical for the survival of *H. pylori* in the human gut. On a detailed analysis of the HPGQs in the metal-binding proteins, we observed the presence of various G-quadruplex motif in the four genes which are involved in Nickel transportation. Briefly, the open reading frame (ORF) of Nickel permease *nixA* (HP1077) harbored six motifs, five in the same direction as that of the gene while one in the antisense strand. An ABC transporter involved in nickel transportation, *niuD* (HP0889), also harbored eight GQ motifs in the sense strand while one in the anti-sense strand of the gene. *H. pylori* contains two nickel binding periplasmic proteins, *niuB1* (HP1561) and *niuB2* (HP1562) (Shaik et al., 2014). The sequences of both of these genes share 89% sequence similarity and modulate nickel affinity. The GQ mining in these two genes revealed the presence of six GQs in the ORF of *niuB1* and seven in *niuB2*.

Thereafter, we selected one HPGQs each from the above four nickel transport system genes on the basis of cG score obtained from our in-house HPGQ prediction script and PENGUINN score. The HPGQ motif in the ORF region of *nixA* gene (HPGQ1) with a highest cG (160) and PENGUINN score (0.95) was selected for biophysical characterization. Likewise, one HPGQ of ABC transporter *niuD* (HPGQ2) with cG score 140 and PENGUINN score 0.798 was also selected. One HPGQ each of *niuB1* (HPGQ3, cG score = 110, PENGUINN score 0.783) and *niuB2* (HPGQ4,

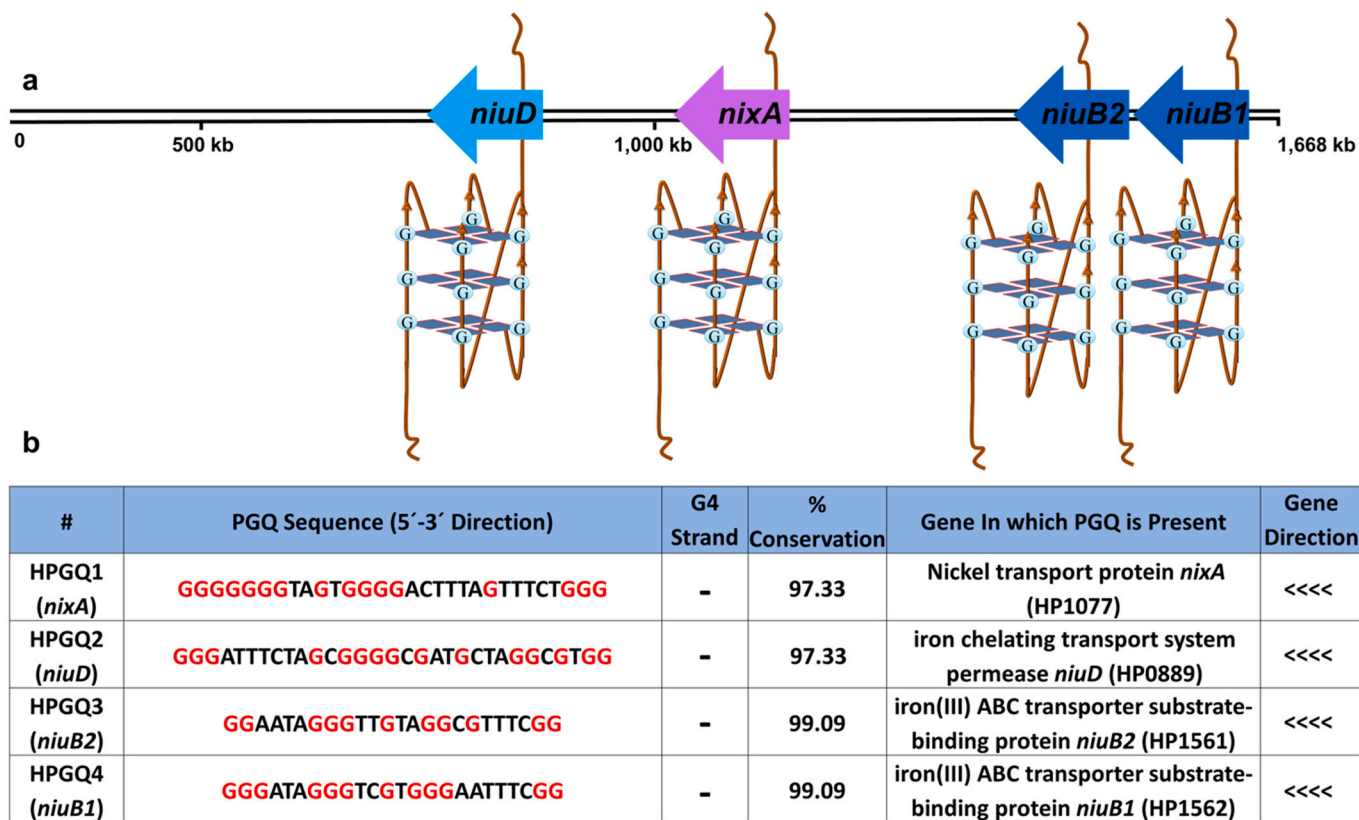


Fig. 2. G-quadruplex motifs in nickel transport associated genes of the *Helicobacter pylori*. (a) Schematic location of G-quadruplex motifs in the *H. pylori* genome. (b) List of G-quadruplexes in the permease proteins of *H. pylori* involved in Nickel transport along with their genomic locations (>>>> Sense strand; <<<<< Anti-sense strand).

cG score = 120, PENGUINN score 0.926) were also selected for further analysis (Fig. 2a). The G-quadruplex motif formation in these nickel transport associated gene was further cross-checked using the QGRS mapper (Supplementary Table S1). Nickel being the virulence determining co-factor in *H. pylori* that plays a critical role in the survival of the pathogen in the acidic environment of the host stomach, we further checked the GQ motif sequence conservedness in the *H. pylori* genus.

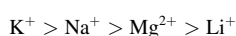
On exploring the motif sequence in all the completely sequenced *H. pylori* genomes, it was observed that the G-tract of the Nickel-associated genes were conserved in the genus. (Supplementary Fig. S2 shows conserved G-tract of the PGQ motifs in the respective genes and Supplementary File S2, having HPGQ motifs location in each strain).

Fig. 2b describes the gene's direction, location, and function, the strand of G-quadruplexes, and conserved frequency of all predicted HPGQs in the *Helicobacter pylori* genome. *nixA* (HP1077) gene encodes a high-affinity membrane nickel transport protein that transports the nickel-metal ion from the periplasmic space to the cytoplasm of the bacteria (Fischer et al., 2016). HPGQ-2 was located in the coding region of the *niuD* (HP0889) gene that encodes an alternative low-affinity nickel transporter protein for the bacteria (Fischer et al., 2016). Though *nixA* and *niuD* are involved in two different pathways for nickel uptake, the inactivation of both of these genes has shown a significant decrease in the intracellular nickel content in the bacteria (Fischer et al., 2016). For the efficient transport of the nickel-metal to the cytoplasm, NiuD utilizes two other periplasmic nickel-binding proteins, NiuB1 (HP1562) and NiuB2 (HP1561) (Fischer et al., 2016). These proteins bind to the nickel-metal present in the periplasmic space and then dock and deliver the nickel metal to the NiuD transporter. Our bioinformatics analysis revealed the presence of two HPGQs (HPGQ3 and HPGQ4) in the coding region of both of these permeases.

Nickel is the key virulence factor for the *H. pylori* pathogenesis enabling the bacteria to survive in the gastric epithelial and mucosa of the host (Benoit et al., 2013) and inhibition of either urease/ dehydrogenase activity or nickel deficient condition showed to be lethal to this bacteria (Fischer et al., 2016). Previously, the presence of the G4 structure in the coding regions has been reported to reduce the expression of particular genes in various pathogens (Mishra et al., 2019; Jain et al., 2020). Also, G-quadruplex motifs negatively regulates the nitrite assimilation in *Paracoccus denitrificans*. Therefore, the G-quadruplex formation in the coding region of nickel transporters might be involved in nickel assimilation inside the *H. pylori* by regulating their expression leading to reduced bacterial survival and virulence inside the stomach of humans and thus represents conserved drug targets for developing active anti-bacterial drugs. Therefore we characterized these G-quadruplex motifs by using various biophysical and biomolecular techniques.

3.2. Circular dichroism spectra and CD melting analysis affirmed the formation of stable G-quadruplex in the conserved PGQs present in the nickel transport-associated genes

Circular dichroism is one of the most reliable techniques to characterize the formation of G-quadruplex structures. G-quadruplex motifs form diverse topologies depending on the loop length and its composition. They have been reported to form parallel, anti-parallel or mixed conformations under different physiological conditions (Supplementary Fig. S3). The positive peak at ~260 nm and a negative peak at ~240 nm corresponds to a parallel G-quadruplex topology, while a positive peak at ~290 nm and a negative peak at ~260 nm represent an anti-parallel G-quadruplex topology (Kypr et al., 2009). However, the mix or hybrid G-quadruplex shows two positive signals at 260 nm and 290 nm and a negative signal at 240 nm (Kypr et al., 2009). The cations can place themselves in between the G-tetrads or along the plane of G-tetrads and provide additional stability to the G-quadruplex structure. The ranking of the stabilizing ability of the well-studied cations is as below:



Therefore, we analyzed the CD spectra of each HPGQs in the presence of these four cations, namely K^+ , Na^+ , Mg^{2+} and Li^+ cations. Since *H. pylori* survive at low pH (~4.5) and grow at neutral pH (~7.0) in the human stomach, we assessed the ability of G-quadruplex formation in HPGQs motifs at both low and neutral pH. CD spectra analysis suggested the formation of the G-quadruplex topologies by each HPGQs at both low pH and neutral pH (Fig. 3 and Supplementary Fig. S4). At low pH, HPGQ1 formed a mixed-hybrid G-quadruplex in all the cations. HPGQ2 majorly formed parallel topology with a little hump at ~290 nm in K^+ and Na^+ . This hump may corresponds to the presence of minor anti-parallel topologies in the presence of these two cations. In Li^+ and Mg^{2+} , HPGQ2 formed parallel topology. HPGQ3 formed mixed hybrid topologies, while HPGQ4 formed parallel topologies in all the four cations. Similar results were also observed at neutral pH (Fig. S4).

All the HPGQs at low and neutral pH, showed the highest ellipticity in the presence of K^+ cation, affirming the most stable G-quadruplex formation in the cation (Bhattacharyya et al., 2016). Also, bacteria have an efficient potassium homeostasis system and can tolerated hundreds of millimolar concentrations of K^+ ions (Martinac et al., 2008). Therefore, we further assessed the effect of increasing K^+ ion concentration (50 mM up to 200 mM) on the HPGQ topologies. As anticipated, the increasing concentration of the K^+ cation provided additive stability to each of the HPGQs, as was observed with the increase in the molar ellipticity (See Supplementary Fig. S5) (Largy et al., 2016).

To further assess the thermodynamic stability of each HPGQs in the absence and presence of various cations, we performed CD melting analysis. Consistent with CD spectra studies, thermal denaturation analysis also showed the higher stability of G-quadruplex in the presence of K^+ cation as compared with the other cations (Fig. 4 and Supplementary Fig. S6).

3.3. Nuclear magnetic resonance (NMR) confirmed the formation of G-quadruplex structures in the HPGQ motifs

NMR spectroscopy can be used to confirm the formation of the G-quadruplex structure by DNA and RNA. The guanine imino protons involved in G-quadruplex structure formation exhibit the characteristic signal between 10-12 ppm, while the protons involved in the Watson-crick bonds gave peaks at 12-14 ppm (Adrian et al., 2012). Therefore, we performed the proton NMR (1H NMR) experiment to confirm the G4 folding of all four HPGQs at both the low (~4.5) and neutral pH (~7.0) *in vitro*. All the four HPGQs exhibited a chemical shift signal between 10 to 12 ppm and evident in the formation of the G-quadruplex structure (Fig. 5 and Supplementary Fig. S7).

3.4. Electrophoretic mobility shift assay corroborates the formation of intramolecular G-quadruplex by HPGQs

We have used an electrophoretic mobility shift assay (EMSA) to monitor the electrophoretic mobility of all the HPGQs was monitored on native PAGE and examined compared to their linear counterparts. The electrophoretic mobility of the given molecule provides evidence about their molecularity and the presence of multimeric conformation. A well-known *Tel22* intramolecular G-quadruplex forming DNA along with its linear counterpart was taken as a positive control. In comparison to the linear oligo of the same size and length, the fast-migrating species are considered to form intramolecular topology, while relatively slow migrating species are supposed to form an intermolecular G-quadruplex structure. All the DNA sequences were incubated in the buffers containing different monovalent ions and were resolved by a native PAGE. In comparison to the linear oligo of the same size and length, the fast-migrating species are considered to form intramolecular topology, while relatively slow migrating species are supposed to form an intermolecular G-quadruplex structure. The results (Supplementary Fig. S8) show that all the HPGQs (lanes 4-7) migrated faster than their linear counterpart (lane 3 and 8) indicating the formation of the

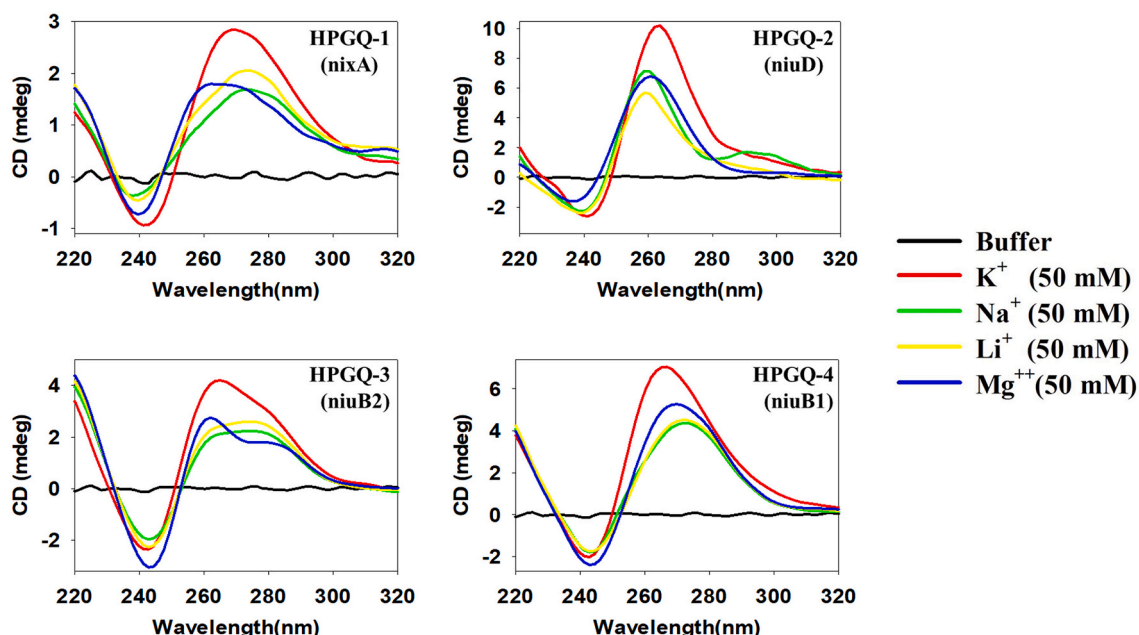


Fig. 3. Circular Dichroism spectra of Nickel transport associated HPGQs: CD spectra analysis in the presence of Ammonium acetate buffer (10 mM) (pH = 4.5) containing either of 50 mM KCl (red), 50 mM NaCl (green), 50 mM LiCl (yellow) or 50 mM MgCl₂ (blue). (For interpretation of the references to colour in this figure legend, the reader is referred to the web version of this article.)

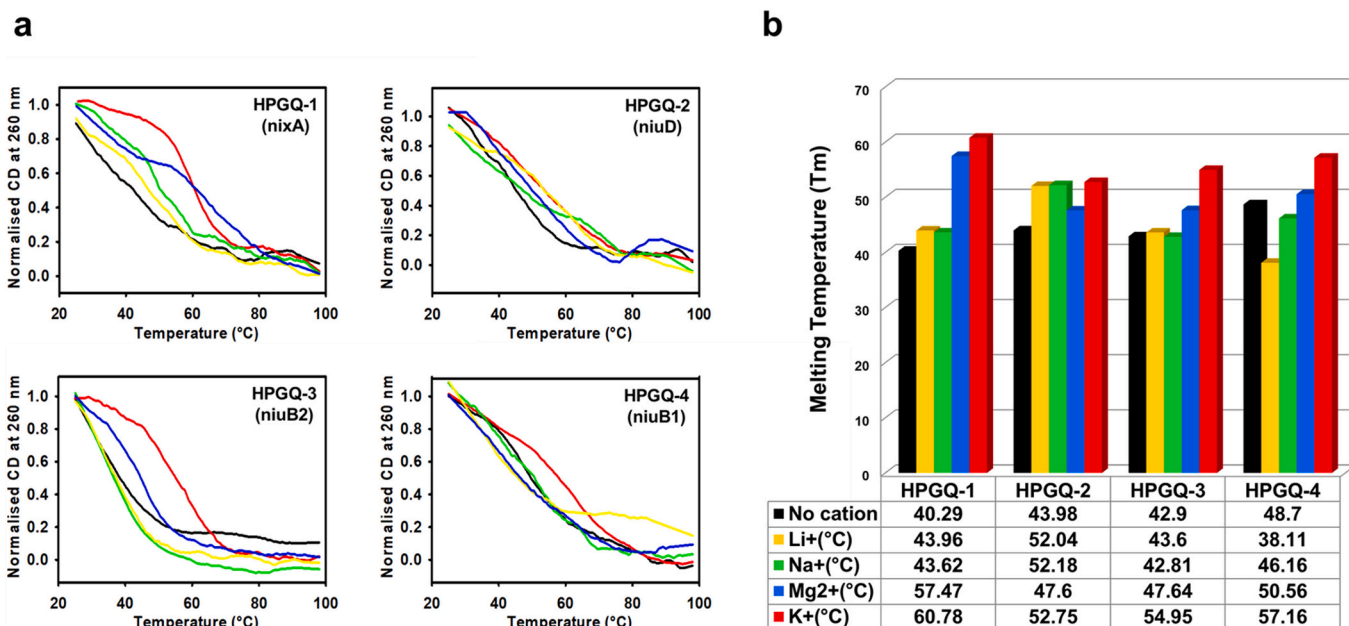


Fig. 4. Thermal denaturation Analysis: (a) CD Melting spectra in the presence of ammonium acetate buffer (10 mM) (pH = 4.5) in the absence of any cation (Black) or in the presence of four different buffers [K⁺ (Red), Na⁺ (Green), Li⁺ (Yellow) and Mg²⁺ (Blue)] for the putative Ni²⁺ permease G-quadruplex sequences predicted in *Helicobacter pylori*. (b) Melting temperature (T_m) of the four HPGQs. (For interpretation of the references to colour in this figure legend, the reader is referred to the web version of this article.)

intramolecular G-quadruplex topology.

3.5. G-quadruplex ligand stabilizes the HPGQs by an energetically favorable interaction

G-quadruplex binding ligands have been investigated for their therapeutic potential for affecting the stability of the G-quadruplex structure. TMPyP4 was observed to stabilize the human telomeric G-quadruplex structure and thereby hold anti-cancer properties (Zheng

et al., 2016). TMPyP4 has also been shown to stabilize the G-quadruplex present in the L gene that encodes for the viral RNA-dependent RNA polymerase in the Ebola virus. Further, the stabilization of this particular G-quadruplex structure showed to inhibit the expression of the gene product (Wang et al., 2016) Its inhibition stops the viral RNA processing inside the host cell (Wang et al., 2016). TMPyP4 also inhibited the *Mycobacterium tuberculosis* growth in the micromolar range and reduced the expression of G-quadruplex harboring genes (Mishra et al., 2019). Similarly, PhenDC3, a known G-quadruplex ligand, stabilizes the G-

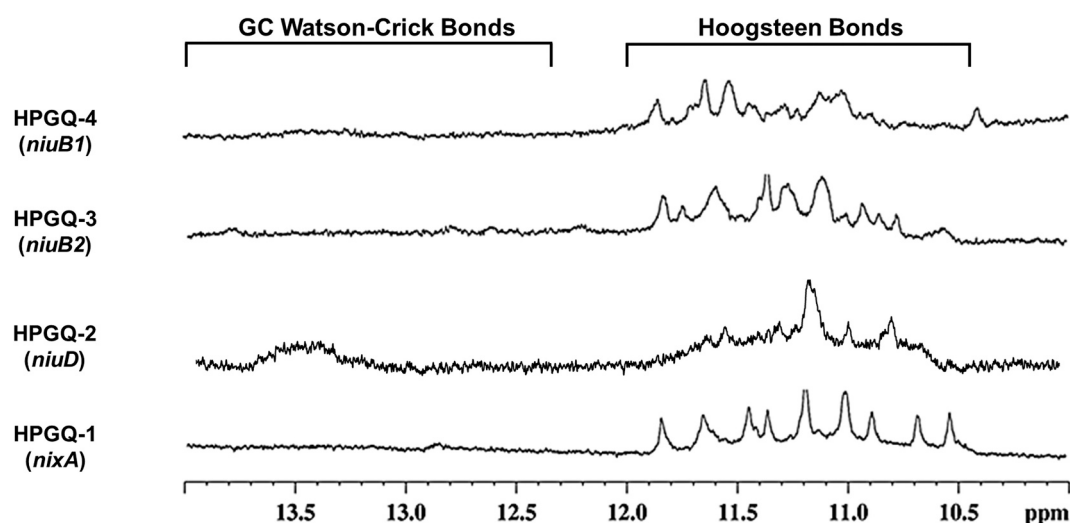


Fig. 5. NMR Spectra. ^1H NMR spectra of Nickel transport associated HPGQs in the presence of K^+ ion at acidic pH (4.5).

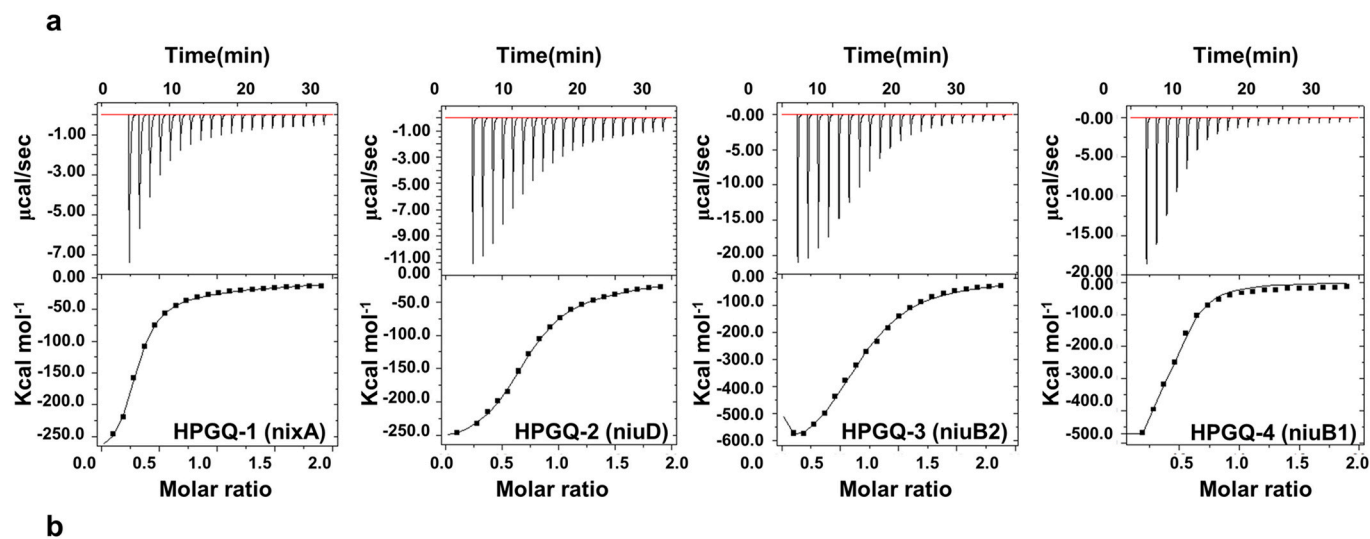
quadruplex motif present in the terminal region of the KSHV genome (Madireddy et al., 2016). It eventually obstructs the movement of the replication fork and inhibits the replication of the KSHV genome inside the host cell (Madireddy et al., 2016). Recently, another G-quadruplex specific binder, BRACO-19, has been shown to kill the *M. tuberculosis* bacteria *in vivo* by stabilizing the G-quadruplex motifs present in the bacterial genome (Perrone et al., 2017b).

In accordance with the above findings, here, we sought to investigate the interaction of TMPyP4 with the HPGQs by isothermal titration calorimetry (ITC) (Fig. 6). ITC analysis revealed the energetically favorable interaction between TMPyP4 and HPGQs by exhibiting a decrease in the change in enthalpy (ΔH) in every reaction (Du et al., 2016). The change in enthalpy and association constant for each set of

the reaction are shown in Fig. 6a. The measured association constant (K_a) was observed in the micromolar (μM) range that suggested the high affinity of the TMPyP4 for the HPGQs (Fig. 6b).

3.6. TMPyP4 stabilizes the HPGQ leading to a decrease in the expression of the mTFP gene

HPGQ motifs were cloned just upstream of the start codon of the mTFP gene in the pCAG-mTFP plasmid. The cloned GQ plasmids, was transfected in HEK293T cells line and treated with the increasing concentration of TMPyP4. We observed a decrease in the fluorescence intensity of TMPyP4 treated cells as compared to the untreated ones. This occurred due to decline in the expression of the mTFP gene because of



Thermodynamic parameters	HPGQ1 (nixA)	HPGQ2 (niuD)	HPGQ3(niuB1)	HPGQ4(niuB2)
$\Delta\text{H1}(\text{cal/mol})$	-2.885E5	-2.716E5	-4.825E5	-4.389E5
$K_a1 (\text{M}^{-1})$	1.59E6	2.84E6	5.00E7	1.00E6
$\Delta\text{H2} (\text{cal/mol})$	-4.760E7	-5.051E4	-7.164E5	-4.702E5
$K_a2 (\text{M}^{-1})$	2.79E4	8.41E4	4.54E5	6.74E13

Fig. 6. Conserved G-quadruplex interaction with a G-quadruplex binder TMPyP4. (a) Two mode binding ITC thermograms of HPGQs with TMPyP4. (b) Change in enthalpies and the association constant values obtained from two-mode binding with TMPyP4 for each HPGQ.

the stabilization of G-quadruplex structure by TMPyP4 binding. No effect was observed in the mutated one (Fig. 7).

4. Discussion

The transition metal atoms have been recognized for their role in the survival of the bacteria during the latent or active phase of infection in the host (Becker and Skaar, 2014). Interestingly, the Nickel atom was identified as a co-factor for the two essential enzymes (urease and [Ni-F] hydrogenase) of *H. pylori* bacteria that help the bacteria to survive in a variety of pH range (Fischer et al., 2016; De Reuse et al., 2013b). The pathogenicity of the *H. pylori* in humans depends on their ability to import the nickel-metal atom from the stomach linings (Kusters et al., 2006). A recent study reported the increased eradication rate of *H. pylori* upon having the nickel-free diet (Campanale et al., 2014). For the efficient acquisition of the Nickel-metal, *H. pylori* possess a nickel transportation system that includes the following players (Fig. 8) (Fischer et al., 2016):

An outer membrane nickel transporter: FrpB4

Two inner membrane nickel permease: NixA and NiuD

Two periplasmic nickel-binding proteins: NiuB1 and NiuB2

G-quadruplex motifs present in the genome of the human pathogens have been revealed to regulate the expression of the harboring genes and alter their pathogenicity (Ruggiero and Richter, 2018; Harris and Merrikk, 2015). As well, G-quadruplex structure acts as a negative regulators of nitrate assimilation in *P. denitrificans*. Heterotrophic bacteria can use NO_3^- as a key nitrogen source for cell growth. *P. denitrificans* have a highly dedicated system to assimilate the NO_3^- and is coded by the *nasABGHC* operon. The *nasT* gene that act as a cis regulator for the expression of *nasABGHC* operon has a G-quadruplex motif in the promoter region. This G-quadruplex, when stabilized with G-quadruplex specific ligand TMPyP4 and a benzophenoxazine derivative 1, decrease

in the gene expression of the *nasABGHC* operon. Also, a decrease in cell growth was observed when the bacteria were grown in NO_3^- dependent manner but no difference was seen in NH_4^+ dependent growth (Waller et al., 2016). This clearly demonstrated the role of G-quadruplex in the regulation of nitrate assimilation in the bacterium. With this study, we are presenting the first report on the presence of highly conserved G-quadruplex motifs in the nickel transportation system of *H. pylori* using in-silico analysis and their formation were ascertained by various bio-physical techniques. Our study highlights the identification and characterization of the four G-quadruplex motifs involved in this nickel transportation system of the *H. pylori* bacteria. The four genes involved in nickel transportation, namely, *nixA*, *niuD*, *niuB1* and *niuB2* harbour various G-quadruplex motifs in its ORF region (Fig. 8). The presence of distinct imino-proton peaks in 1D ^1H NMR spectra corroborated the formation of G-quadruplex structure and their topologies were displayed by CD spectra of these HPGQs. In addition, the formation of intramolecular G-quadruplex structures were affirmed by EMSA experiments. The intramolecular G-quadruplexes have been observed to work as a cis-regulatory site during the replication, recombination, and gene expression (Parrotta et al., 2014); therefore, the formation of the intramolecular G-quadruplex topology may work as promising drug targets for developing therapeutics against *H. pylori* infection. Moreover, ITC was performed to study the affinity of the known G-quadruplex binding ligand (TMPyP4) with the G-quadruplex motifs. Inhibiting the expression of nickel transporter genes may lead to reduced transportation of nickel metal in the bacterial cytoplasm and eventually inactivating the bacterial enzymes essential for the survival of the bacteria inside the host (Fig. 8). Also, a decrease in the fluorescence intensity of transfected HEK293 cells upon addition of TMPyP4 further affirmed the formation of stable G-quadruplex conformation by the four HPGQs that inhibited the expression of mTFP protein. Furthermore, pharmacological targeting of these conserved G-quadruplex motifs by a small

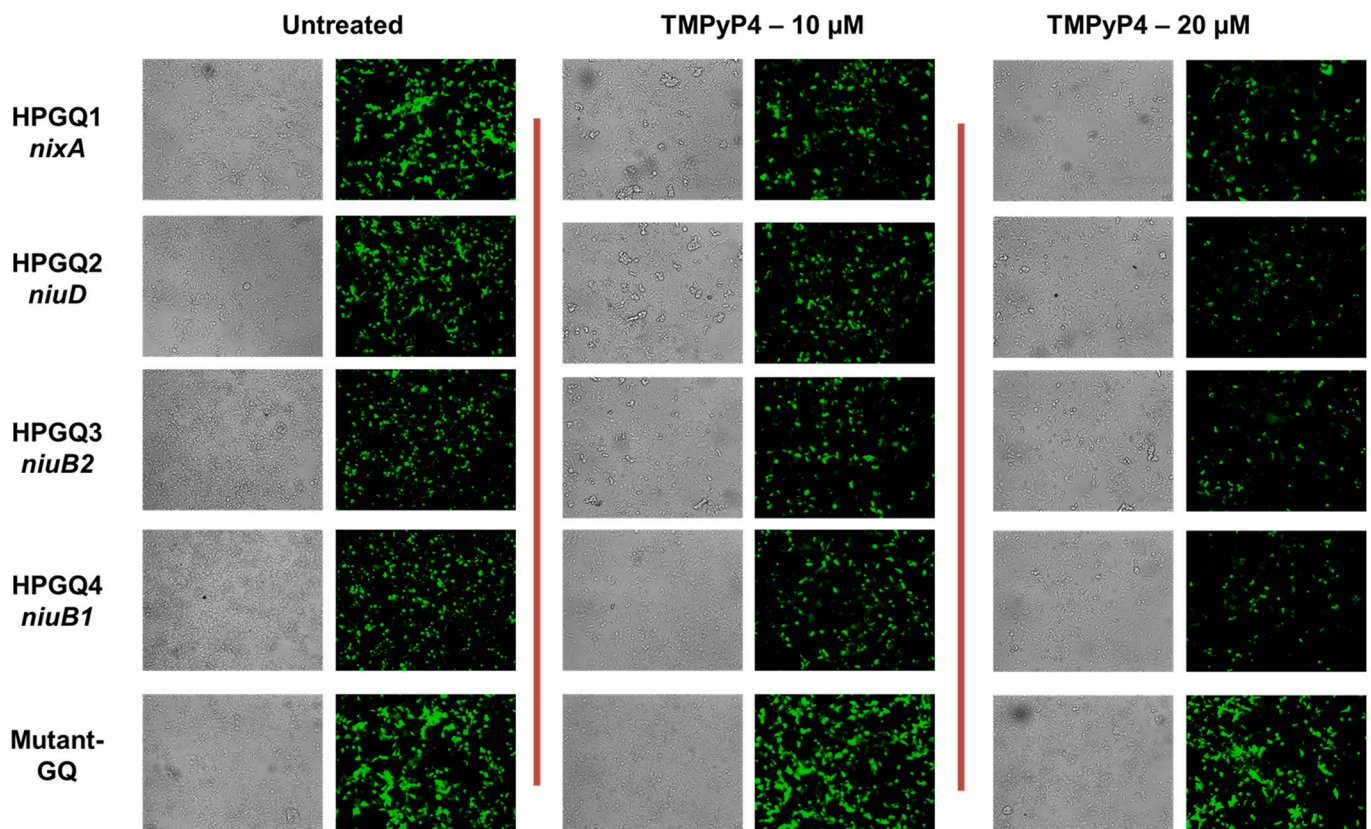


Fig. 7. mTFP based reporter assay. Fluorescence images of HEK293 cells transfected with HPGQ-pCAG-mTFP and Mutant-GQ-pCAG-mTFP plasmids in the absence or presence of TMPyP4 (10 μM and 20 μM).

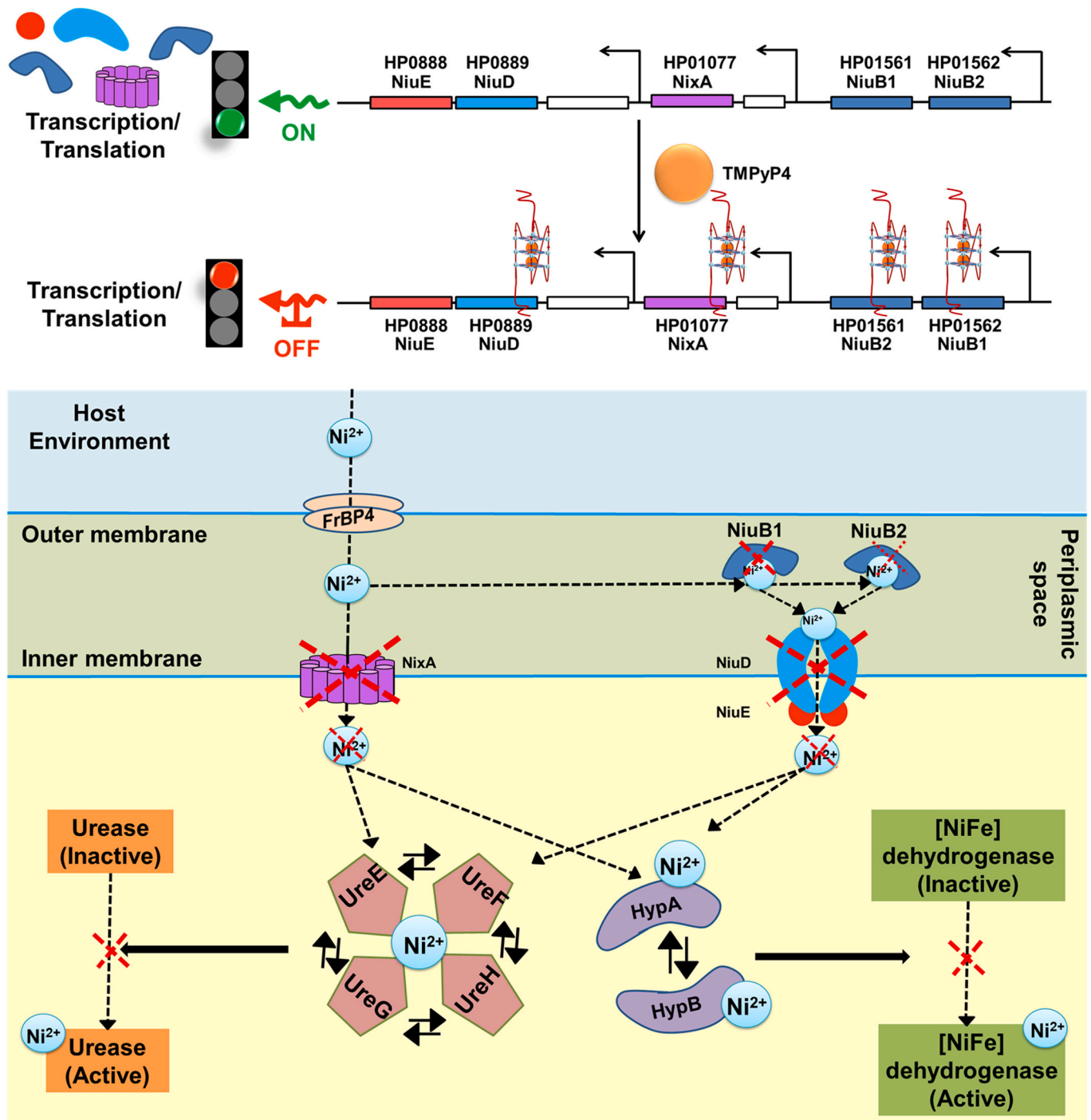


Fig. 8. Schematic representation of G-quadruplex motifs in Nickel transport associated genes and their functions. (a) Nickel permease genes clusters involved in the influx of Nickel from the periplasmic space to the cytoplasm. Addition of TMPyP4 may lead to the stabilization of G-quadruplexes in *nixA*, *niuD*, *niuB1*, and *niuB2* resulting in the inhibition of transcription and translation of their respective proteins. (b) Diagrammatic representation of the location and function of Nickel permeases which leads to activation of Urease and [NiFe] dehydrogenase enzymes essential for *Helicobacter pylori* survival and virulence in the host environment.

molecule is anticipated for combating drug resistance problems in *H. pylori* infection.

5. Conclusion

Our preliminary analysis revealed the genome of *H. pylori* has large number of motifs that have a high propensity to form G-quadruplex motifs. Functional annotation revealed the presence of G-quadruplex motifs in the large number of essential genes, including those involved in

metabolic pathways, nucleotide binding, metal binding *etc.* In genes coding for metal-binding proteins Nickel transport associated genes showed the presence of highly conserved G-quadruplex motifs. As Nickel homeostasis is critical for the activation of Urease and [NiFe] dehydrogenase required for the survival and growth of *H. pylori* in the human gastric environment, we explored four HPGQs associated with these nickel transporters by performing *in-vitro* analysis. Various biophysical techniques affirmed the formation of stable G-quadruplex motifs in various cations, especially K⁺ ion, while reporter-based assay showed

the formation of stable motifs inside the cells. As G-quadruplex motifs are used as therapeutic targets in various cancers, neurological diseases, and viral pathogenesis, we believe that this new finding of putative G-quadruplex structures within the *H. pylori* genome can open new domains of disease treatment against this pathogenic bacterium and helps in combating other related diseases.

Competing interests

The authors declare no competing interests.

Authors' contributions

A.K. conceived, designed, and analyzed the experiments. Bioinformatics analysis was done by U.S., and N.J. US performed the experiments. US, SKM, NJ, AK analyzed the data and wrote the main manuscript. MS reviewed by AK, AT and PY.

Credit author statement

Conceptualization, Experiment designed, Analysis: Amit Kumar; Bioinformatics analysis.

and Experiment: Uma Shankar and Neha Jain; Manuscript writing: Amit Kumar, Uma.

Shankar, Neha Jain, Subodh Kumar Mishra; Result Analysis: Amit Kumar, Uma Shankar, Neha Jain, Subodh Kumar Mishra ; Review and Editing: Amit Kumar, Uma Shankar, Neha Jain, Subodh Kumar Mishra, Arpita Tawani, Puja Yadav.

Acknowledgments

The authors are thankful to the Sophisticated Instrumentation Facility at IIT Indore for CD and NMR experiments. The pCAG-mTFP plasmid was a kind gift of Dr. Debasis Nayak, Associate professor, IIT, Indore, India. US acknowledge MHRD, New Delhi, and NJ is thankful to CSIR, New Delhi, for their SRF fellowships. PY thanks the Science and Engineering Research Board, Department of Science and Technology, India for providing the grant [ECR/2015/000431].

Appendix A. Supplementary data

Supplementary data to this article can be found online at <https://doi.org/10.1016/j.meegid.2022.105298>.

References

- Adrian, M., Heddi, B., Phan, A.T., 2012. NMR spectroscopy of G-quadruplexes. *Methods* 57 (1), 11–24.
- Alsulaimany, F.A.S., et al., 2020. Prevalence of *Helicobacter pylori* infection and diagnostic methods in the Middle East and North Africa Region. *Medicina (Kaunas)* 56 (4).
- Artusi, S., Ruggiero, E., 2021. Antiviral activity of the G-quadruplex ligand TMPyP4 against Herpes Simplex Virus-1. *3* (2).
- Awadasseid, A., et al., 2021. G-quadruplex stabilization via small-molecules as a potential anti-cancer strategy. *Biomed. Pharmacother.* 139, 111550.
- Backert, S., et al., 2016. Pathogenesis of *Helicobacter pylori* infection. *Helicobacter* 21 (Suppl. 1), 19–25.
- Bartas, M., et al., 2019. The presence and localization of G-quadruplex forming sequences in the domain of bacteria. *Molecules* 24.
- Bartas, M., et al., 2020. In-depth bioinformatic analyses of nidovirales including human SARS-CoV-2, SARS-CoV, MERS-CoV viruses suggest important roles of non-canonical nucleic acid structures in their lifecycles. *Front. Microbiol.* 11, 1583.
- Becker, K.W., Skaar, E.P., 2014. Metal limitation and toxicity at the interface between host and pathogen. *FEMS Microbiol. Rev.* 38 (6), 1235–1249.
- Benoit, S.L., Miller, E.F., Maier, R.J., 2013. *Helicobacter pylori* stores nickel to aid its host colonization. *Infect. Immun.* 81 (2), 580–584.
- Bezzi, G., et al., 2021. CNBP binds and unfolds in vitro G-quadruplexes formed in the SARS-CoV-2 positive and negative genome strands. *22* (5).
- Bhattacharyya, D., Mirihana Arachchilage, G., Basu, S., 2016. Metal cations in G-quadruplex folding and stability. *Front. Chem.* 4 (38).
- Biswas, B., Kumari, P., Vivekanandan, P., 2018. Pac1 Signals of Human Herpesviruses Contain a Highly Conserved G-Quadruplex Motif.

- Bohálová, N., et al., 2021. Analyses of viral genomes for G-quadruplex forming sequences reveal their correlation with the type of infection. *Biochimie* 186, 13–27.
- Bohálová, N., Cantara, A., Bartas, M., Kaura, P., Štátný, J., Pečinka, P., Fojta, M., Brázda, V., et al., 2019. Tracing dsDNA Virus–Host Coevolution through Correlation of Their G-Quadruplex-Forming Sequences. *Int. J. Mol. Sci.* 22, 3433. <https://doi.org/10.3390/ijms22073433>.
- Brázda, V., et al., 2019. G4Hunter web application: a web server for G-quadruplex prediction. *Bioinformatics* 35 (18), 3493–3495.
- Brázda, V., et al., 2021. G-quadruplexes in H1N1 influenza genomes. *BMC Genomics* 22 (1), 77.
- Butovskaya, E., et al., 2019. HIV-1 nucleocapsid protein unfolds stable RNA G-quadruplexes in the viral genome and is inhibited by G-quadruplex ligands. *ACS Infect. Dis.* 5 (12), 2127–2135.
- Cahoon, L.A., Seifert, H.S., 2009. An alternative DNA structure is necessary for pilin antigenic variation in *Neisseria gonorrhoeae*. *Science* 325 (5941), 764–767.
- Campanale, M., et al., 2014. Nickel free-diet enhances the *Helicobacter pylori* eradication rate: a pilot study. *Dig. Dis. Sci.* 59 (8), 1851–1855.
- Chen, B.J., et al., 2014. Small molecules targeting c-Myc oncogene: promising anti-cancer therapeutics. *Int. J. Biol. Sci.* 10 (10), 1084–1096.
- de Reuse, H., Vinella, D., Cavazza, C., 2013a. Common themes and unique proteins for the uptake and trafficking of nickel, a metal essential for the virulence of *Helicobacter pylori*. *Front. Cell. Infect. Microbiol.* 3, 94.
- De Reuse, H., Vinella, D., Cavazza, C., 2013b. Common themes and unique proteins for the uptake and trafficking of nickel, a metal essential for the virulence of *Helicobacter pylori*. *Front. Cell. Infect. Microbiol.* 3 (94).
- Dey, U., et al., 2021. G-quadruplex motifs are functionally conserved in cis-regulatory regions of pathogenic bacteria: an in-silico evaluation. *Biochimie* 184, 40–51.
- Dhapola, P., Chowdhury, S., 2016. QuadBase2: web server for multiplexed guanine quadruplex mining and visualization. *Nucleic Acids Res.* 44 (W1), W277–W283.
- Ding, Y., Fleming, A.M., Burrows, C.J., 2018. Case studies on potential G-quadruplex-forming sequences from the bacterial orders Deinococcales and Thermales derived from a survey of published genomes. *Sci. Rep.* 8 (1), 15679.
- Domanovich-Asor, T., et al., 2021. Unraveling antimicrobial resistance in *Helicobacter pylori*: global resistome meets global phylogeny. *Helicobacter* 26 (2), e12782.
- Du, X., et al., 2016. Insights into protein–ligand interactions: mechanisms, models, and methods. *Int. J. Mol. Sci.* 17 (2), 144.
- Endoh, T., Kawasaki, Y., Sugimoto, N., 2013. Suppression of gene expression by G-quadruplexes in open reading frames depends on G-quadruplex stability. *Angew. Chem. Int. Ed. Engl.* 52 (21), 5522–5526.
- Fischer, F., et al., 2016. Characterization in *Helicobacter pylori* of a nickel transporter essential for colonization that was acquired during evolution by gastric *Helicobacter* species. *PLoS Pathog.* 12 (12), e1006018.
- Fleming, A.M., et al., 2016. Zika virus genomic RNA possesses conserved G-quadruplexes characteristic of the Flaviviridae family. *ACS Infect. Dis.* 2 (10), 674–681.
- Harris, L.M., Merrick, C.J., 2015. G-quadruplexes in pathogens: a common route to virulence control? *PLoS Pathog.* 11 (2), e1004562.
- Holder, I.T., Hartig, J.S., 2014. A matter of location: influence of G-quadruplexes on *Escherichia coli* gene expression. *Chem. Biol.* 21 (11), 1511–1521.
- Hooi, J.K.Y., et al., 2017. Global prevalence of *Helicobacter pylori* infection: systematic review and meta-analysis. *Gastroenterology* 153 (2), 420–429.
- Huang da, W., Sherman, B.T., Lempicki, R.A., 2009a. Systematic and integrative analysis of large gene lists using DAVID bioinformatics resources. *Nat. Protoc.* 4 (1), 44–57.
- Huang da, W., Sherman, B.T., Lempicki, R.A., 2009b. Bioinformatics enrichment tools: paths toward the comprehensive functional analysis of large gene lists. *Nucleic Acids Res.* 37 (1), 1–13.
- Huang, M.J., et al., 2006. A small-molecule c-Myc inhibitor, 10058-F4, induces cell-cycle arrest, apoptosis, and myeloid differentiation of human acute myeloid leukemia. *Exp. Hematol.* 34 (11), 1480–1489.
- Huppert, J.L., Balasubramanian, S., 2005. Prevalence of quadruplexes in the human genome. *Nucleic Acids Res.* 33 (9), 2908–2916.
- Jain, N., et al., 2020. G-quadruplex stabilization in the ions and maltose transporters gene inhibit *Salmonella enterica* growth and virulence. *Genomics* 112 (6), 4863–4874.
- Jain, Neha, Shankar, Uma, 2022. Conserved G-Quadruplex Motifs Regulate Gene Expression in *Neisseria meningitidis*. *ACS Infect. Dis.* 8 (4), 728–743. <https://doi.org/10.1021/acinfecdis.1c00383>.
- Kikin, O., D'Antonio, L., Bagga, P.S., 2006. QGRS Mapper: a web-based server for predicting G-quadruplexes in nucleotide sequences. *Nucleic Acids Res.* 34 (Web Server issue), W676–W682.
- Klimentova, E., et al., 2020. PENGUINN: precise exploration of nuclear G-quadruplexes using interpretable neural networks. *Front. Genet.* 11 (1287).
- Kuryavyi, V., et al., 2012. RecA-binding p1E G4 sequence essential for pilin antigenic variation forms monomeric and 5' end-stacked dimeric parallel G-quadruplexes. *Structure* 20 (12), 2090–2102.
- Kusters, J.G., van Vliet, A.H.M., Kuipers, E.J., 2006. Pathogenesis of *Helicobacter pylori* infection. *Clin. Microbiol. Rev.* 19 (3), 449–490.
- Kypr, J., et al., 2009. Circular dichroism and conformational polymorphism of DNA. *Nucleic Acids Res.* 37 (6), 1713–1725.
- Largy, E., et al., 2016. Quadruplex turncoats: cation-dependent folding and stability of quadruplex-DNA double switches. *J. Am. Chem. Soc.* 138 (8), 2780–2792.
- Lista, M.J., et al., 2017. Nucleolin directly mediates Epstein-Barr virus immune evasion through binding to G-quadruplexes of EBNA1 mRNA. *Nat. Commun.* 8, 16043.
- Madireddy, A., et al., 2016. G-quadruplex-interacting compounds alter latent DNA replication and episomal persistence of KSHV. *Nucleic Acids Res.* 44 (8), 3675–3694.

- Majee, P., et al., 2020a. Identification and characterization of two conserved G-quadruplex forming motifs in the Nipah virus genome and their interaction with G-quadruplex specific ligands. *Sci. Rep.* 10 (1), 1477.
- Majee, P., et al., 2020b. Genome-wide analysis reveals a regulatory role for G-quadruplexes during adenovirus multiplication. *Virus Res.* 283, 197960.
- Majee, P., et al., 2021. Inhibition of Zika virus replication by G-quadruplex-binding ligands. *Mol. Ther. Nucl. Acid* 23, 691–701.
- Martinac, B., Saimi, Y., Kung, C., 2008. Ion channels in microbes. *Physiol. Rev.* 88 (4), 1449–1490.
- Mégraud, F., 2012. The challenge of *Helicobacter pylori* resistance to antibiotics: the comeback of bismuth-based quadruple therapy. *Ther. Adv. Gastroenterol.* 5 (2), 103–109.
- Mishra, S.K., et al., 2016. G4IPDB: a database for G-quadruplex structure forming nucleic acid interacting proteins. *Sci. Rep.* 6, 38144.
- Mishra, S.K., et al., 2019. Characterization of G-quadruplex motifs in *espB*, *espK*, and *cyp51* genes of *Mycobacterium tuberculosis* as potential drug targets. *Mol. Ther. Nucl. Acid* 16, 698–706.
- Murat, P., Balasubramanian, S., 2014. Existence and consequences of G-quadruplex structures in DNA. *Curr. Opin. Genet. Dev.* 25, 22–29.
- Pandya, N., et al., 2021. Curcumin analogs exhibit anti-cancer activity by selectively targeting G-quadruplex forming c-myc promoter sequence. *Biochimie* 180, 205–221.
- Parrotta, L., et al., 2014. Targeting unimolecular G-quadruplex nucleic acids: a new paradigm for the drug discovery? *Expert Opin. Drug Discovery* 9 (10), 1167–1187.
- Perrone, R., et al., 2014. Anti-HIV-1 activity of the G-quadruplex ligand BRACO-19. *J. Antimicrob. Chemother.* 69 (12), 3248–3258.
- Perrone, R., et al., 2017a. Mapping and characterization of G-quadruplexes in *Mycobacterium tuberculosis* gene promoter regions. *Sci. Rep.* 7 (1), 5743.
- Perrone, R., et al., 2017b. Mapping and characterization of G-quadruplexes in *Mycobacterium tuberculosis* gene promoter regions. *Sci. Rep.* 7 (1), 5743.
- Reznichenko, O., et al., 2019. Novel cationic bis(acylhydrazones) as modulators of Epstein–Barr virus immune evasion acting through disruption of interaction between nucleolin and G-quadruplexes of EBNA1 mRNA. *Eur. J. Med. Chem.* 178, 13–29.
- Rhodes, D., Lipps, H.J., 2015. G-quadruplexes and their regulatory roles in biology. *Nucleic Acids Res.* 43 (18), 8627–8637.
- Ruggiero, E., Richter, S.N., 2018. G-quadruplexes and G-quadruplex ligands: targets and tools in antiviral therapy. *Nucleic Acids Res.* 46, 3270–3283.
- Ruggiero, E., et al., 2019. Stable and conserved G-quadruplexes in the long terminal repeat promoter of retroviruses, 5 (7), 1150–1159.
- Saha, T., et al., 2019. *Mycobacterium tuberculosis* UvrD1 and UvrD2 helicases unwind G-quadruplex DNA. *FEBS J.* 286 (11), 2062–2086.
- Shaik, M.M., et al., 2014. *Helicobacter pylori* periplasmic receptor CeuE (HP1561) modulates its nickel affinity via organic metallophores. *Mol. Microbiol.* 91 (4), 724–735.
- Shalaby, T., et al., 2013. G-quadruplexes as potential therapeutic targets for embryonal tumors. *Molecules* 18 (10), 12500–12537.
- Shankar, U., et al., 2020a. Exploring computational and biophysical tools to study the presence of G-quadruplex structures: a promising therapeutic solution for drug-resistant *Vibrio cholerae*. *Front. Genet.* 11, 935.
- Shankar, U., et al., 2020b. Conserved G-quadruplex motifs in gene promoter region reveals a novel therapeutic approach to target multi-drug resistance *Klebsiella pneumoniae*. *Front. Microbiol.* 11 (1269).
- Sidebotham, R.L., et al., 2003. How *Helicobacter pylori* urease may affect external pH and influence growth and motility in the mucus environment: evidence from in-vitro studies. *Eur. J. Gastroenterol. Hepatol.* 15 (4), 395–401.
- Tawani, A., et al., 2016. Evidences for Piperine inhibiting cancer by targeting human G-quadruplex DNA sequences. *Sci. Rep.* 6, 39239.
- Tawani, A., Mishra, S.K., Kumar, A., 2017. Structural insight for the recognition of G-quadruplex structure at human c-myc promoter sequence by flavonoid Quercetin, 7 (1), 3600.
- Thakur, R.S., et al., 2014. *Mycobacterium tuberculosis* DinG is a structure-specific helicase that unwinds G4 DNA: implications for targeting G4 DNA as a novel therapeutic approach. *J. Biol. Chem.* 289 (36), 25112–25136.
- Waller, Z.A.E., et al., 2016. Control of bacterial nitrate assimilation by stabilization of G-quadruplex DNA. *Chem. Commun. (Camb.)* 52 (92), 13511–13514.
- Wang, S.R., et al., 2016. Chemical targeting of a G-quadruplex RNA in the Ebola virus L gene. *Cell. Chem. Biol.* 23 (9), 1113–1122.
- Wroblewski, L.E., Peek Jr., R.M., Wilson, K.T., 2010. *Helicobacter pylori* and gastric cancer: factors that modulate disease risk. *Clin. Microbiol. Rev.* 23 (4), 713–739.
- Wu, F., et al., 2021. Genome-wide analysis of DNA G-quadruplex motifs across 37 species provides insights into G4 evolution, 4 (1), 98.
- Yadav, P., et al., 2021. G-Quadruplex structures in bacteria: biological relevance and potential as an antimicrobial target. *J. Bacteriol.* 203 (13), e0057720.
- Yu, Y., Ouyang, Y., Yao, W., 2018. shinyCircos: an R/shiny application for interactive creation of Circos plot. *Bioinformatics* 34 (7), 1229–1231.
- Zheng, X.H., et al., 2016. TMPyP4 promotes cancer cell migration at low doses, but induces cell death at high doses. *Sci. Rep.* 6, 26592.